NIH Public Access
Author Manuscript
Arch Biochem Biophys. Author manuscript; available in PMC 2012 August 15.

Published in final edited form as:
Arch Biochem Biophys. 2011 August 15; 512(2): 183–189. doi:10.1016/j.abb.2011.05.015.

Redox reactions of the FAD-containing apoptosis-inducing factor (AIF) with quinoidal xenobiotics: a mechanistic study

Lina Misevičienė[a], **Žilvinas Anusevičius**[a], **Jonas Šarlauskas**[a], **Irina F. Sevrioukova**[b], and **Narimantas Čėnas**[a,*]

[a] Institute of Biochemistry of Vilnius University, Mokslininkų 12, LT-08662 Vilnius, Lithuania

[b] Department of Molecular Biology and Biochemistry, University of California, Irvine, CA 92697-3900, USA

Abstract

Mitochondrial apoptosis-inducing factor (AIF) is a FAD-containing protein that under certain conditions translocates to the nucleus and causes a programmed cell death, apoptosis. The apoptogenic action of AIF is redox controlled as the NADH-reduced AIF dimer has lower affinity for DNA than the oxidized monomer. To gain further insights into the mechanism of AIF, we investigated its interaction with a series of quinone oxidants, including a number of anticancer quinones. Our data indicate that the NADH:quinone oxidoreduction catalyzed by AIF follows a "ping-pong" scheme, with the reductive half-reaction being rate-limiting and the $FADH^-$-NAD^+ charge-transfer complex serving as an electron donor. AIF is equally reactive toward benzo- and naphthoquinones, but may discriminate structures with a higher number of aromatic rings. The reactivity of quinones is mainly defined by their one-electron reduction potential, whereas the size and nature of the substituents play a minor role. AIF is unlikely to significantly contribute to bioreductive activation of low-potential quinoidal anticancer quinones. However, high-potential quinones, *e.g.* a toxic natural compound naphthazarin, maintain AIF in the oxidized state when a significant excess of NADH is present. Thus, these compounds may prevent the accumulation of the reduced form of AIF *in vivo*, and enhance AIF-mediated apoptosis.

Keywords

Apoptosis-inducing factor; quinone; apoptosis induction; oxidative stress; bioreductive activation

Apoptosis-inducing factor (AIF) is a FAD-containing protein tethered to the inner membrane of mitochondria in normal cells. There is compelling evidence that AIF plays a vital role in mitochondrial bioenergetics but its specific redox function is still unknown [1]. Another well established role of AIF is induction of caspase-independent programmed cell death, apoptosis [2,3]. Upon outer mitochondrial membrane permeabilization, mature AIF undergoes proteolysis [4-6] and the truncated fragment (AIF(Δ1-101/102)) translocates to the cytosol and subsequently to the nucleus to trigger chromatin condensation and DNA degradation [2,7,8].

© 2011 Elsevier Inc. All rights reserved.

*Corresponding author: Fax + 370-5-2729196. narimantas.cenas@bchi.vu.lt.

This paper is dedicated to Professor Liuda Rasteikienė on the occasion of her 85th birthday

Publisher's Disclaimer: This is a PDF file of an unedited manuscript that has been accepted for publication. As a service to our customers we are providing this early version of the manuscript. The manuscript will undergo copyediting, typesetting, and review of the resulting proof before it is published in its final citable form. Please note that during the production process errors may be discovered which could affect the content, and all legal disclaimers that apply to the journal pertain.

NIH-PA Author Manuscript
NIH-PA Author Manuscript
NIH-PA Author Manuscript

NIH-PA Author Manuscript

NIH-PA Author Manuscript

NIH-PA Author Manuscript

AIF has a glutathione reductase (GR) fold and is most similar to bacterial oxygenase-coupled ferredoxin reductases [9,10]. This and the presence of the FAD cofactor suggested that AIF is a redox active protein. The earlier studies showed that when refolded and reconstituted with FAD, AIF possesses modest NAD(P)H:acceptor oxidoreductase activities, but the flavin cofactor is not required for the apoptotic action [2,3,9,11]. However, recent functional and structural studies performed on naturally folded AIF demonstrated that its oligomeric and conformational states change upon FAD oxidoreduction, which in turn could affect the apoptogenic action [12, 13]. In particular, it was found that reduction of AIF by NAD(P)H leads to formation of a dimer with a tight $FADH^-$-$NAD(P)^+$ charge-transfer (CT) complex, resistant to oxidation by oxygen and interacting with DNA weaker than the oxidized monomer. Furthermore, the CT complex has a differently folded regulatory loop and an inaccessible nuclear leading sequence, through which AIF is predominantly transported to the nucleus. Altogether, these findings indicated that the apoptogenic function of AIF might be redox controlled [12,13]. It is important therefore to further investigate the redox properties and reactions catalyzed by AIF, especially with the redox active cytotoxic compounds, as they may affect the cell-death-inducing potency of the flavoprotein.

Since translocation of AIF from mitochondria is facilitated under the ‘oxidative stress’ conditions [14,15], it is logical to suggest that interaction of AIF with reactive oxidative species could shift the redox equilibrium toward the oxidized monomeric state, thereby enhancing proapoptotic properties of AIF. This possibility prompted us to reexamine reactions of AIF with quinoidal compounds, which have previously been poorly and randomly characterized [2,3,9,11,12], and include in the study a series of quinoidal antitumour agents. It is well known that quinones can become toxic upon reduction by flavoenzymes, and induce apoptotic and necrotic cell death [16-18]. The ‘oxidative stress’-type cytotoxicity arises from the redox cycling of their radical forms produced after one-electron reduction by flavin-containing electrontransferases, *e.g.* NADPH:cytochrome P450 reductase [16,19,20]. On the other hand, two-electron reduction of antitumour aziridinyl-substituted quinones by mammalian NAD(P)H: quinone oxidoreductase (NQO1), leads to formation of the corresponding hydroquinones that alkylate DNA more readily than the parent oxidized compounds [20,21]. Apart from the possible role of the aforementioned reactions in AIF-mediated apoptosis, investigation of the AIF-quinone interaction is interesting from a mechanistic viewpoint, because the reduced active center of AIF contains a tightly bound NAD^+ (K_d = 5–80 nM [12], and Churbanova and Sevrioukova, unpublished data) which is sandwiched between the near-coplanar isoalloxazine ring of $FADH^-$ and aromatic ring of Phe309 [13]. This makes AIF an interesting experimental model for studying flavin-dependent transformations of redox active compounds.

In this study, we characterized the quinone reductase mechanism and substrate specificity of a model form (AIF(Δ1-77)) of mature mouse AIF, which possesses the same redox potential and NADH:acceptor reductase activities as a recombinant mature AIF [12], by measuring steady- and pre-steady-state kinetics of electron transfer to various quinones, including toxic natural compounds and quinoidal antitumour agents with different electron-accepting potency and steric parameters.

Materials and methods

Expression and purification of recombinant mouse AIF(Δ1-77) were carried out as described previously [12]. AIF concentration was determined spectrophotometrically using ε_{452} = 13.2 $mM^{-1}cm^{-1}$. NADH, NAD^+, cytochrome *c*, superoxide dismutase, ubiquinone-6, and model quinones (compounds 1, 2, 4-6, 10-15, 18-21, 24; Fig. 1) were obtained from Sigma-Aldrich. Daunorubicin was from Minmedprom (Russia). Antitumour aziridinyl-substituted 1,4-benzoquinones AZQ, MeDZQ, RH1 and BZQ (compounds 7, 16, 17, 23; Fig. 1) were

NIH-PA Author Manuscript

NIH-PA Author Manuscript

NIH-PA Author Manuscript

synthesized as described previously [21-23]. *t*-Butyl-substituted 1,4-benzoquinones (compounds 3, 8, 9; Fig. 1) were synthesized as reported elsewhere [24,25]. The purity of synthesized compounds was checked according to their melting point, elemental analysis, IR and NMR spectra.

Steady-state kinetic measurements were carried out in 0.1 M K-phosphate (pH 7.0) containing 1 mM EDTA at 25 °C using a Hitachi-557 UV-VIS spectrophotometer. The reaction was monitored spectrophotometrically by following consumption of 200 μM NADH ($\Delta\varepsilon_{340}$ = 6.2 mM^{-1} cm^{-1}) at various electron acceptor concentrations in 1.0 cm optical path cells. In some cases, higher concentrations of NADH and 0.2 cm optical path cells were used. Experiments with ubiquinone-6 (50 μM maximal concentration) were performed in the presence of 0.1% Triton X-100. Reduction of 50 μM cytochrome *c* was monitored at 550 nm ($\Delta\varepsilon_{550}$ = 20 mM^{-1} cm^{-1}). Catalytic (k_{cat}) and bimolecular rate constants (k_{cat}/K_m) for the quinone reduction at fixed NADH concentrations, or NADH oxidation at fixed quinone concentrations correspond to the reciprocal intercepts and slopes of the Lineweaver-Burk plots, [E]/*v vs.* 1/[oxidant] or [E]/v *vs.* [NADH], where [E] is the enzyme concentration, and *v* is the reaction rate. k_{cat} is the number of NADH molecules oxidized by a single enzyme molecule per second. The calculated rates were corrected for the intrinsic NADH-oxidase activity of AIF, 0.0003 s^{-1}. In case of 1,4-benzoquinone and 2-methyl-1,4-benzoquinone, the reaction rates were also corrected for non-enzymatic oxidation of NADH by these compounds. In control experiments, kinetic measurements were performed in a sealed anaerobic cuvette under argon atmosphere. Kinetic parameters were obtained by Quasi-Newton or Simplex-Quasi-Newton nonlinear estimation methods using Statistica (version 4.30, StatSoft, 1993).

Pre-steady-state kinetic studies on AIF were performed under aerobic conditions at 25 °C in 0.1 M K-phosphate (pH 7.0) containing 1 mM EDTA, using a SX.17 MV stopped-flow spectrophotometer (Applied Photophysics). Absorbance changes were monitored at 452 and 700 nm to follow FAD reduction and $FADH^-$-NAD^+ charge-transfer complex formation, respectively [12]. In the AIF reduction experiments, 40-50 μM protein was rapidly mixed with an equal volume of an excess of NADH, and the absorbance changes at 452 and 700 nm were recorded. In the AIF reoxidation experiments, 30-50 μM AIF was first mixed with sub-equimolar NADH (95 %) and when the 452 and 700 nm absorbance stabilized (35-40 min), the reduced AIF-NAD^+ complex was rapidly mixed with an equal volume of 2,6-dimethyl-1,4-benzoquinone solution, and absorbance changes at 452 and 700 nm were recorded. In multiple turnover experiments, AIF was rapidly mixed with an equal volume of solution containing both NADH and quinone. Control reoxidation experiments were performed under anaerobic conditions, where the solutions of quinones and NADH before the introduction of AIF were purged with ultrapure argon for 60 min and loaded into the stopped flow apparatus in gas-tight syringes. Kinetic data were analyzed using the Applied Photophysics software.

Results

Reduction of AIF by NADH is accompanied by a decrease in absorbance at 452 nm and appearance of a long-wavelength absorbance band (Fig. 2), indicative of the $FADH^-$-NAD^+ CT complex formation. The latter species is produced as a result of π-π interactions between the reduced isoalloxazine ring of FAD and electron-defficient nicotinamide ring of the reaction product, NAD^+. This type of spectra has been observed for the $FADH^-$ -$NAD(P)^+$ complexes of reduced lipoamide dehydrogenase and glutathione reductase, formed in the presence of alkylating agents which modify the catalytic thiols of the aforementioned enzymes [26]. The semiquinone form of AIF is thermodynamically unstable and does not accumulate during the reoxidation of NADH-reduced AIF at pH 7.0 [12]. However, during

NIH-PA Author Manuscript

NIH-PA Author Manuscript

NIH-PA Author Manuscript

the reoxidation of reduced AIF-NAD^+ complex by oxygen at pH ≥8.0, a small amount (10-15%) of anionic semiquinone ($FAD^{\cdot-}$, λ_{max} = 380 nm) was formed (Churbanova and Sevrioukova, unpublished data). Due to high affinty of reduced AIF for NAD^+ (K_d = 5-80 nM [12]; Churbanova and Sevrioukova, unpublished data) and low reactivity of the $FADH^-$-NAD^+ species toward oxygen (half-lifetime under air atmosphere >120 min [12]), all experiments described below were performed under aerobic conditions, unless specified otherwise.

Steady-State Kinetics

Steady-state reduction of 2,6-dimethyl-1,4-benzoquinone by AIF follows a “ping-pong” scheme, as evidenced by parallel Lineweaver-Burk plots at fixed concentrations of NADH and different quinone concentrations (Fig. 3). The calculated bimolecular rate constant (k_{cat}/K_m) of AIF reduction by NADH was equal to 280±20 $M^{-1}s^{-1}$, whereas the k_{cat} value at saturating concentrations of NADH and quinone oxidant was estimated to be 0.24±0.02 s^{-1}, consistent with the previous findings [12]. The reaction rates measured under anaerobic conditions were the same, whithin experimental error.

In order to evaluate the specificity of AIF for quinones, we examined a series of compounds with a broad range of quinone/semiquinone redox potential (E^1_7, 0.09 ÷ -0.41 V), and different number of aromatic rings (benzo-, naphtho-, and anthraquinones) and size of substituents, as reflected by the Van der Waals volume (VdWvol) (Fig. 1, Table 1). The studied compounds included antitumour aziridinyl-substituted 1,4-benzoquinones AZQ, BZQ, MeDZQ, and RH1, and daunorubicin, as well as quinoidal products of oxidation of *t*-butyl-substituted-1,4-hydroquinone antioxidants (Fig. 1, Table 1). The presence of high concentrations of NAD^+ (5.0 mM) had a weak inhibiting effect, decreasing k_{cat}/K_m for the quinone reduction by less than 15%. When plotted against the E^1_7 value for benzo- and naphthoquinones (Fig. 4), log k_{cat}/K_m linearly increased with an increase in the electron-accepting potency of the compounds (r^2 = 0.776, F(1.18) = 62.34). On the other hand, tricyclic anthraquinones and daunorubicin were less reactive toward AIF as might be expected based on their E^1_7 values (Fig. 4). Comparison of reactivities of RH1, MeDZQ, and 1,4-dihydroxy-9,10-anthraquinone, which have similar Van der Waals volumes (Table 1), suggests that the low reactivity of tricyclic quinones is not attributed to their larger size. However, when VdWvol was used as a second variable in a two-parameter regression analysis, statistics for the kinetic data on benzo- and naphthoquinones (compounds 1-17, 19, 23, 24; Table 1) was slightly improved (r^2 = 0.782, F(2.17) = 35.06) and a weak negative influence of VdWvol on their reactivity became evident:

$$\log k_{cat}/K_m = (4.2458 \pm 0.2725) + (4.7106 \pm 0.6553) E^1_7 - (0.0021 \pm 0.0014)\ \text{VdWvol.} \quad (1)$$

Similarly, a large VdWvol might be a reason for the lack of reactivity of ubiquinone-6 (E^1_7 = -0.24 V, VdWvol = 727 Å^3), which we tested as a possible physiological oxidant of AIF. It can be concluded, therefore, that (i) AIF is equally specific toward benzo- and naphthoquinones but may discriminate structures with a higher number of aromatic rings, and (ii) the reactivity of benzo- and naphthoquinones is mainly defined by their oxidative potency, while the size and nature of their substituents play a less important role. Similar log *k vs.* E^1_7 dependences are characteristic for a number of flavoenzymes which reduce quinones either in one-electron way (NADPH:cytochrome P-450 reductase, ferredoxin:$NADP^+$ reductase), or in two-electron way (*Enterobacter cloacae* nitroreductase, *E. cloacae* PB2 pentaerythritol reductase) [20,27].

NIH-PA Author Manuscript

NIH-PA Author Manuscript

NIH-PA Author Manuscript

Quantitatively, the percentage of a one-electron flux during NAD(P)H:quinone oxidoreduction can be estimated using the 1,4-benzoquinone-mediated enzymatic reduction of cytochrome *c*. At pH < 7.2, cytochrome *c* is reduced by 1,4-benzohydroquinone with a negligibly low rate, whereas 1,4-benzosemiquinone delivers electrons to the hemoprotein very rapidly ($k = 10^6$ $M^{-1}s^{-1}$ [28]). Hence, the percentage of a one-electron flux can be expressed as a ratio of the cytochrome *c* reduction rate and the doubled rate of enzymatic oxidation of NAD(P)H in the presence of 1,4-benzoquinone [28]. AIF was found to reduce quinones in a mixed one- and two-electron way, with 34±5.0 % of a one-electron flux.

Pre-steady-state Kinetics

We also examined the pre-steady-state kinetics of AIF reactions. A 452 nm absorbance decrease and an increase at 700 nm observed during reduction of AIF by NADH (Fig. 2) proceed with similar rates (Fig. 5A). The rate constant for AIF reduction reaches the limiting value at high concentrations of NADH (Fig. 5B), which was equal to 0.31±0.03 s^{-1} under studied conditions. The estimated apparent bimolecular reduction rate constant was 251±20 $M^{-1}s^{-1}$, close to the k_{cat}/K_m value derived from the steady-state kinetic data (Fig. 3). Besides, the rate constant for the pre-steady-state AIF reduction with 200 μM NADH (Fig. 5B) is in the same range as the k_{cat} values for the quinone reduction reactions measured under steady-state conditions with a similar NADH concentration (Table 1). Again, the presence of 5.0 mM NAD^+ had no feasible effect on the kinetics of AIF reduction (Fig. 5B).

During pre-steady-state oxidation of reduced AIF by 2,6-dimethyl-1,4-benzoquinone, an increase in absorbance at 452 nm and a decrease at 700 nm proceed with similar rates (Fig. 6A). This means that NAD^+ dissociation/CT complex decay occur simultaneously with the FAD oxidation. The rate constant for AIF oxidation depends linearly on the 2,6-dimethyl-1,4-benzoquinone concentration, reaching values that exceed the maximal rate for the NADH-dependent AIF reduction by one order of magnitude (Figs. 5B and 6B). The bimolecular oxidation rate constant for the 2,6-dimethyl-1,4-benzoquinone, in turn, is close to the corresponding value obtained in the steady-state kinetic experiments ($8.0±0.5 \times 10^3$ $M^{-1}s^{-1}$ and $1.2 ±0.5 \times 10^4$ $M^{-1}s^{-1}$, respectively). Although formation of the FAD semiquinone may be anticipated during the single-electron oxidation of AIF, we observed neither a biphasic nature of the absorbance changes nor a transient increase at 380 nm, indicative of formation of $FAD^{\cdot -}$ as a reaction intermediate. The reoxidation reactions carried out under anaerobic conditions gave identical within error results at 452, 700, and 380 nm, comparing to those obtained under aerobic conditions.

Next we examined how the AIF redox state changes during turnover with NADH under conditions imitating the cytotoxic action of quinones in mammalian cells. It was found that even at low cytotoxic concentration of quinones, 20 μM [16], and significant excess of NADH over quinone, 5,8-dihydroxy-1,4-naphthoquinone and 2,6-dimethyl-1,4-benzoquinone significantly delay formation of the reduced form of the flavoprotein, as judged from the kinetics of the absorbance decay at 452 nm (Fig. 7). In the presence of RH1, on the other hand, the course of the reaction was only weakly perturbed, with AIF being predominantly in the reduced state (Fig. 7). Although a stoichiometric quinone:AIF ratio was used, AIF performed multiple turnovers (Fig. 7). This is due to regeneration of the oxidants under aerobic conditions. Free radicals and, presumably, two-electron reduced 5,8-dihydroxy-1,4-naphthoquinone formed during a mixed one- and two-electron reduction of quinones by AIF, are rapidly reoxidized by oxygen [16]. In the absence of external oxygen supply, reoxidation of AIF in the reaction mixture terminates after oxygen depletion.

NIH-PA Author Manuscript

NIH-PA Author Manuscript

NIH-PA Author Manuscript

Discussion

The goal of this study was to characterise the mechanism of reduction of quinoidal xenobiotics and drugs by mitochondrial AIF with emphasis on its possible contribution to apoptosis or other toxic events in the cell. First, we characterized the catalytic cycle of NADH:quinone oxidoreduction mediated by AIF. The steady-state reactions catalyzed by AIF follow a “ping-pong” mechanism (Fig. 3) and involve the reductive and oxidative half-reactions. One notable observation is that the maximal pre-steady-state rate of NADH-dependent FAD reduction (0.31±0.03 s^{-1}, Fig. 5B) is close to the maximal turnover rate under steady-sate conditions (0.24±0.02 s^{-1}) but considerably lower than the rate of AIF oxidation by 2,6-dimethyl-1,4-benzoquinone (Fig. 6B). Our results suggest that (i) the reductive half-reaction is rate-limiting, (ii) quinones are predominantly reduced by the $FADH^-$-NAD^+ CT complex, and (iii) FAD oxidation coincides with NAD^+ dissociation. That the oxidized pyridine nucleotide weakly binds to oxidized AIF and rapidly and irreversibly dissociates upon FAD oxidation is evidenced by the finding that high concentrations of NAD^+ do not interfere with AIF reduction with NADH (Fig. 5A). The proposed reaction course is shown in Scheme 1 (E_o and E_r correspond to the oxidized and reduced forms of AIF; S, P, Q_o and Q_r stand for NADH, NAD^+, oxidized and reduced quinone, respectively), while the steady-state reaction rate consistent with the “ping-pong” mechanism can be described by Equation 2:

$$\frac{[E]}{v}=\frac{1}{k_2}+\frac{k_{-1}+k_2}{k_1k_2[S]}+\frac{1}{k_3[Q_o]} \quad (2)$$

Correlation between the reactivity and redox potentials of the investigated quinones (Fig. 4) suggests that AIF has no pronounced specificity for any particular quinone structure, but may discriminate tricyclic quinones and bulky ubiquinone-6 possibly due to sterical hindrances with the active site. The mixed single- and two-electron reduction of quinones by AIF is another indication of instability of the FAD semiquinone [9,12], because two-electron or mixed reduction of quinones is usually performed by the enzymes that do not stabilize flavin radicals [20,29]. The partial single-electron character of quinone reduction does not contradict to the lack of a transient formation of $FAD^{\cdot -}$ in the pre-steady-state oxidation of AIF. This shows that the oxidation of two-electron reduced flavin by the single-electron oxidant is slower than the oxidation of flavin semiquinone by a second molecule of the oxidant, the former reaction being the rate-limiting step in the reoxidation [30].

Secondly, our data demonstrate that the quinone reductase activity of AIF (expressed as a k_{cat}/K_m ratio in Table 1) is 10^2-10^4-fold lower than that of cytochrome P450 reductase and NAD(P)H:quinone oxidoreductase (NQO1) [19-21], the two major producers of one- and two-electron reduced forms of quinone xenobiotics, respectively, that promote coresponding ways of quinone cytotoxicity in mammalian cells [16,20,21]. The quinone reductase activity of AIF is also 10-100-fold lower than that of mammalian thioredoxin reductase [31], but is comparable with the activity of glutathione reductase from various sources [32,33]. This implies that the quinone reductase reactions catalyzed by AIF are unlikely to play a significant role in the bioreductive activation of quinone drugs and xenobiotics *in vivo*. Nonetheless, the interaction of AIF with quinones may be physiologically important, because some of these compounds at low concentrations could significantly delay reduction of FAD even when NADH is in significant excess (Fig. 7). Consequently, by maintaining AIF in the oxidized form, quinones may enhance its proapoptotic properties under reducing conditions. This outcome can be mediated only by the relatively high-potential quinones that oxidize AIF relatively fast (*e.g.*, 5,8-dihydroxy-1,4-naphthoquinone and 2,6-dimethyl-1,4-

NIH-PA Author Manuscript

NIH-PA Author Manuscript

NIH-PA Author Manuscript

benzoquinone), but not by the slowly reacting anticancer compounds with the lower E^1_7 values, such as RH1 (Fig. 7, Table 1).

The low quinone reductase activity of AIF is unlikely to be due to the low redox potential of the FAD/FADH$^-$ couple (E^0_7 = -0.341 V; determined in the absence of NAD(H) [12]), which in general should favor quinone reduction. One possible factor that could affect the AIF reactivity toward oxidants is the FAD redox potential change induced by binding of NAD$^+$. In homologous to AIF putidaredoxin reductase, for example, association of NAD$^+$ elevates E^0_7 by 170 mV [34]. Taking into account the estimated K_d values for the complex between NAD$^+$ and reduced (5–80 nM [12]; Churbanova and Sevrioukova, unpublished data) and oxidized AIF (>10 mM; Fig. 5B), the NAD$^+$-dependent redox potential change calculated from the Nernst equation would be within the 0.165-0.183 V range, giving the E^0_7 value for the reduced AIF-NAD$^+$ complex of -0.158 ÷ -0.176 V. Such drastic E^0_7 change could certainly lower the electron donating ability of the FADH$^-$-NAD$^+$ CT complex. Interestingly, the His453Leu mutant of AIF, which possesses a 56 mV higher E^0_7 (determined in the absence of NAD(H)) but does not form CT complex with NAD$^+$, catalyzes electron transfer reactions more effectively than wild type AIF [13]. Another reason for the low reactivity of AIF could be significant conformational changes occuring during its oxidoreduction. Displacement of Phe309 and the accompanying rearrangement of hydrophobic and H-bonding interactions in the active site during AIF reduction [13] could be energy-consuming and affect the rate of reductive half-reaction. This possibility may explain, in part, why the bimolecular rate constant of AIF reduction with NADH is 10^3-10^5-fold lower compared to that reported for other NAD(P)H-dependent flavoenzymes [21,26,29,31]. In the the oxidative half-reaction, quinones oxidize reduced isoalloxazine ring of FADH$^-$ paralelly stacked with the nicotinamide ring of NAD$^+$, which in turn is shielded by the Phe309 ring [13]. The stacking of three aromatic rings might impede an access of the oxidant to the *re*-face of the isoalloxazine ring and slow down the reaction. The conformational changes in AIF taking place after reduction result in the formation of an aromatic tunnel (Tyr559, Phe507, Tyr 346, Trp350, Trp 578, Tyr491, Phe309, and Phe481) stretching from the active site to the surface [13]. However, this tunnel is unlikely to serve as an access channel for the oxidants because it is too long (>20 Å) and tightly packed. Alternatively, quinones may access the *si*-face of FAD flanked by Pro172, Pro173, Trp195, and Trp482 [13]. This side of the molecule becomes solvent accessible after AIF reduction, although the access to the active site is somewhat hindered by the adjacent 199-202 β-hairpin [13].

In summary, our investigation of the NADH:quinone oxidoreduction catalyzed by AIF revealed that the mitochondrial protein is most reactive toward the high-potential benzo- or naphthoquinones and least reactive toward the low-potential anticancer quinoidal drugs. The quinone reductase activity of AIF is too low to play a significant role in bioreductive activation of quinones *in vivo*. However, some high-potential quinone model compounds or toxic natural compounds like 5,8-dihydroxy-1,4-naphthoquinone (naphthazarin) may affect the redox status of AIF and, thus, modulate its apoptogenic potency by oxidizing the FADH$^-$-NAD$^+$ CT complex. Such potentially harmful AIF-quinone interactions can be exacerbated during oxidative stress and lead to accelerated cell death.

Acknowledgments

This work was supported by the Science and Studies Foundation of Lithuania. I.F.S. was supported by the United States National Institutes of Health Grant GM67637. We thank Prof. Saulius Klimašauskas (Institute of Biotechnology, Vilnius) for the access to stopped-flow facility.

NIH-PA Author Manuscript

NIH-PA Author Manuscript

NIH-PA Author Manuscript

References

1. Hangen E, Blomgren K, Benit P, Kroemer G, Modjtahedi N. Trends Biochem Sci. 2010; 35:278–287. [PubMed: 20138767]
2. Susin SA, Lorenzo HK, Zamzami N, Marzo I, Snow BE, Brothers GM, Magion J, Jacotot E, Costantini P, Loeffler M, Larochette N, Goodlett DR, Aebersold R, Siderowski DP, Penninger JM, Kroemer G. Nature. 1999; 397:441–446. [PubMed: 9989411]
3. Susin SA, Daugas E, Ravagnan L, Samejima K, Zamzami N, Loeffler M, Costantini P, Ferri KF, Irinopoulou T, Prevost MC, Brothers G, Mak TW, Peninger J, Earnshaw WC, Kroemer G. J Exp Med. 2000; 192:571–580. [PubMed: 10952727]
4. Otera H, Ohsakaya S, Nagaura ZI, Ishihara N, Mihara K. EMBO J. 2005; 17:1–12.
5. Polster BM, Basanez G, Etxebarria A, Hardwick JM, Nicholls DG. J Biol Chem. 2005; 280:6447–6454. [PubMed: 15590628]
6. Yuste VJ, Moubarak RS, Delettre C, Bras M, Sancho P, Robert N, d'Alayer J, Susin SA. Cell Death Differ. 2005; 12:1445–1448. [PubMed: 15933737]
7. Wang X, Yang C, Chai J, Shi Y, Xue D. Science. 2002; 298:1587–1592. [PubMed: 12446902]
8. Cande C, Vahsen N, Kouranti I, Schmidt E, Daugas E, Spahr C, Luban J, Kroemer RT, Giordanetto F, Garrido C, Penninger JM, Kroemer G. Oncogene. 2004; 23:1514–1521. [PubMed: 14716299]
9. Miramar MD, Costantini P, Ravagnan L, Saraiva LM, Haouzi D, Brothers G, Penninger JM, Peleato ML, Kroemer G, Susin SA. J Biol Chem. 2001; 276:16391–16398. [PubMed: 11278689]
10. Mate MJ, Ortiz-Lombardia M, Boitel B, Haouz A, Tello D, Susin SA, Penninger J, Kroemer G, Alzari PM. Nat Struct Biol. 2002; 9:442–449. [PubMed: 11967568]
11. Loeffler M, Dougas E, Susin SA, Zamzami N, Metivier D, Nieminen AL, Brothers G, Penninger JM, Kroemer G. FASEB J. 2001; 15:758–767. [PubMed: 11259394]
12. Churbanova IY, Sevrioukova IF. J Biol Chem. 2008; 283:5622–5631. [PubMed: 18167347]
13. Sevrioukova IF. J Mol Biol. 2009; 390:924–938. [PubMed: 19447115]
14. Murahashi H, Azuma H, Zamzami N, Furuya KJ, Ikebuchi K, Yamaguchi M, Yamada Y, Sato N, Fujihara M, Kroemer G, Ikeda H. J Leucocyte Biol. 2003; 73:399–406.
15. Srinivas P, Gopinath G, Banerji A, Dinakar A, Srinavas G. Mol Carcinogenesis. 2004; 40:201–211.
16. O'Brien PJ. Chem-Biol Interact. 1991; 80:1–41. [PubMed: 1913977]
17. Öllinger K, Kågedal K. Subcell Biochem. 2002; 36:151–170. [PubMed: 12037979]
18. Verrax J, Taper H, Buc Calderon P. Curr Mol Pharmacol. 2008; 1:80–92. [PubMed: 20021426]
19. Čėnas N, Anusevičius Ž, Bironaitė D, Bachmanova GI, Archakov AI, Öllinger K. Arch Biochem Biophys. 1994; 315:400–406. [PubMed: 7986084]
20. Čėnas N, Anusevičius Ž, Nivinskas H, Misevičienė L, Šarlauskas J. Methods Enzymol. 2004; 382B:258–277.
21. Anusevičius Ž, Šarlauskas J, Čėnas N. Arch Biochem Biophys. 2002; 404:254–262. [PubMed: 12147263]
22. Winski SL, Hargreaves RHJ, Butler J, Ross D. Clin Cancer Res. 1998; 4:3083–3088. [PubMed: 9865924]
23. Chou F, Khan AH, Driscoll JS. J Med Chem. 1976; 19:1302–1308. [PubMed: 1003407]
24. Karpov VV, Khidekel ML. Zh Org Khim. 1967; 3:1669–1674.
25. McClure JD. J Org Chem. 1963; 28:69–71.
26. Williams, CH, Jr. The Enzymes. 3rd. Boyer, PD., editor. Vol. 13. Academic Press; New York: 1976. p. 89-173.
27. Misevičienė L, Anusevičius Ž, Šarlauskas J, Harris RJ, Scrutton NS, Čėnas N. Acta Biochim Polon. 2007; 54:379–385. [PubMed: 17546202]
28. Iyanagi T, Yamazaki Y. Biochim Biophys Acta. 1970; 216:284–294.
29. Anusevičius Ž, Misevičienė L, Medina M, Martinez-Julvez M, Gomez-Moreno C, Čėnas N. Arch Biochem Biophys. 2005; 437:1444–150.

NIH-PA Author Manuscript

NIH-PA Author Manuscript

NIH-PA Author Manuscript

30. Čėnas N, Diep Le KH, Terrier M, Lederer F. Biochemistry. 2007; 46:4661–4670. [PubMed: 17373777]
31. Čėnas N, Nivinskas H, Anusevičius Ž, Šarlauskas J, Lederer F, Arner ESJ. J Biol Chem. 2004; 279:2583–2592. [PubMed: 14604985]
32. Čėnas NK, Rakauskienė GA, Kulys JJ. Biochim Biophys Acta. 1989; 973:399–404. [PubMed: 2647141]
33. Grellier P, Marozienė A, Nivinskas H, Šarlauskas J, Aliverti A, Čėnas N. Arch Biochem Biophys. 2010; 494:32–39. [PubMed: 19919822]
34. Reipa V, Holden MJ, Vilker VL. Biochemistry. 2007; 46:13235–13244. [PubMed: 17941648]

Abbreviations used

AIF	apoptosis-inducing factor
E^1_7	redox potential of a quinone/semiquinone couple at pH 7.0
E^0_7	redox potential of a quinone/hydroquinone couple (standard potential) at pH 7.0
GR	glutathione reductase
k_{cat}/K_m	bimolecular rate constant
k_{cat}	catalytic constant
AZQ	2,5-bis(carboethoxyamino)-3,6-diaziridinyl-1,4-benzoquinone
BZQ	2,5-bis(2′-hydroxyethylamino)-3,6-diaziridinyl-1,4-benzoquinone
MeDZQ	2,5-dimethyl-3,6-diaziridinyl-1,4-benzoquinone
RH1	2,5-diaziridinyl-3-hydroxymethyl-6-methyl-1,4-benzoquinone
VdWvol	Van der Waals volume

NIH-PA Author Manuscript

NIH-PA Author Manuscript

NIH-PA Author Manuscript

Research Highlights

In this work, we for the first time characterized the catalytic cycle of NADH:quinone reductase reaction of apoptosis-inducing factor (AIF) and characterized its quinone-substrate specificity, which may be important in the potentiation of AIF apoptosis-inducing potency by quinones. We found that low cytotoxic concentrations of quinones may prevent the reduction of AIF even at large excess NADH, thus preventing the formation of reduced AIF, whose dimeric form possesses decreased apoptosis-inducing potency.

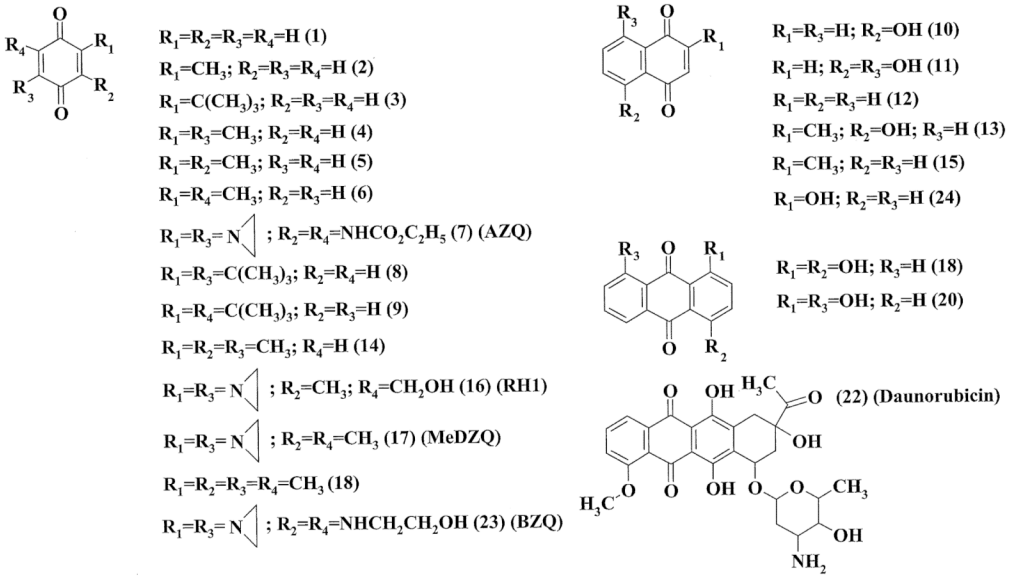

Fig. 1.
Chemical structures of the studied compounds.

NIH-PA Author Manuscript NIH-PA Author Manuscript NIH-PA Author Manuscript

NIH-PA Author Manuscript
NIH-PA Author Manuscript
NIH-PA Author Manuscript

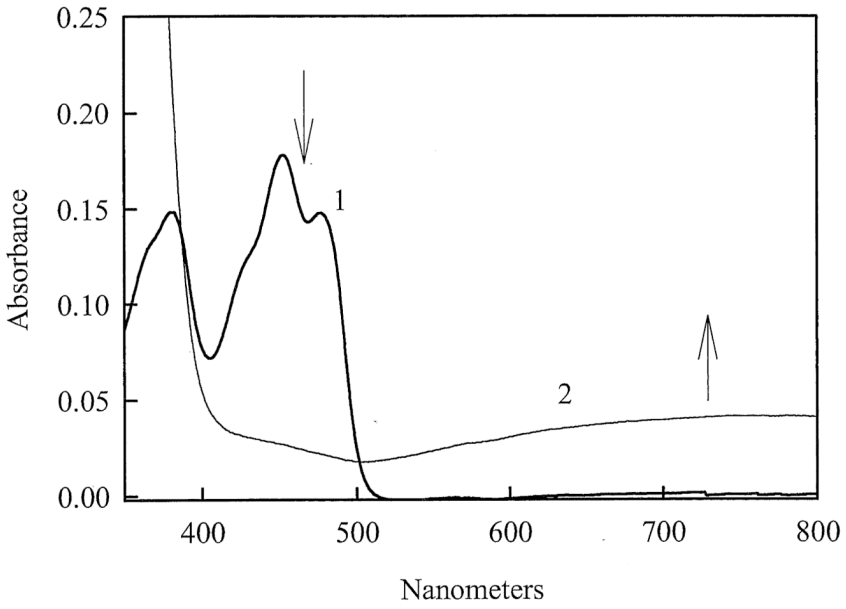

Fig. 2.

Absorbance spectra of 14 μM AIF recorded before (1) and after (2) addition of 140 μM NADH in 100 mM K-phosphate, pH 7.0, 1 mM EDTA at 25 °C.

NIH-PA Author Manuscript

NIH-PA Author Manuscript

NIH-PA Author Manuscript

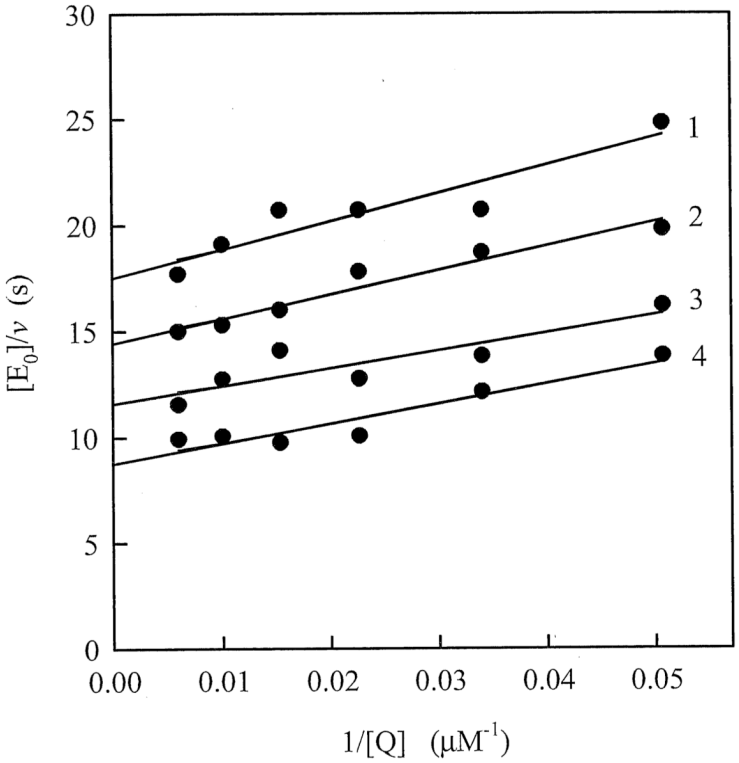

Fig. 3.

Lineweaver-Burk plots of the initial rate constants for NADH oxidation catalyzed by AIF, which were determined at different concentrations of 2,6-dimethyl-1,4-benzoquinone and 216 μM (1), 320 μM (2), 466 μM (3), and 700 μM (4) NADH. Kinetic measurements were conducted in 100 mM K-phosphate, pH 7.0, 1 mM EDTA at 25 °C.

NIH-PA Author Manuscript

NIH-PA Author Manuscript

NIH-PA Author Manuscript

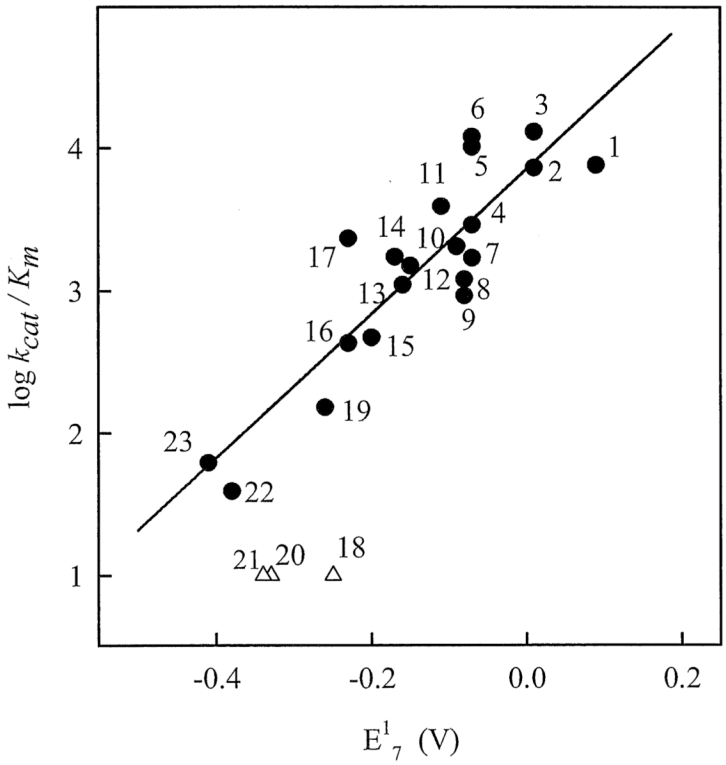

Fig. 4.

Dependence of the reactivity of quinones (log k_{cat}/K_m) toward AIF on their one-electron reduction potential (E^1_7). Quinone numbering is according to Figure 1. The regression line is a linear fit reflecting correlation between the reactivities and E^1_7 values of benzo- and naphthoquinones.

NIH-PA Author Manuscript
NIH-PA Author Manuscript
NIH-PA Author Manuscript

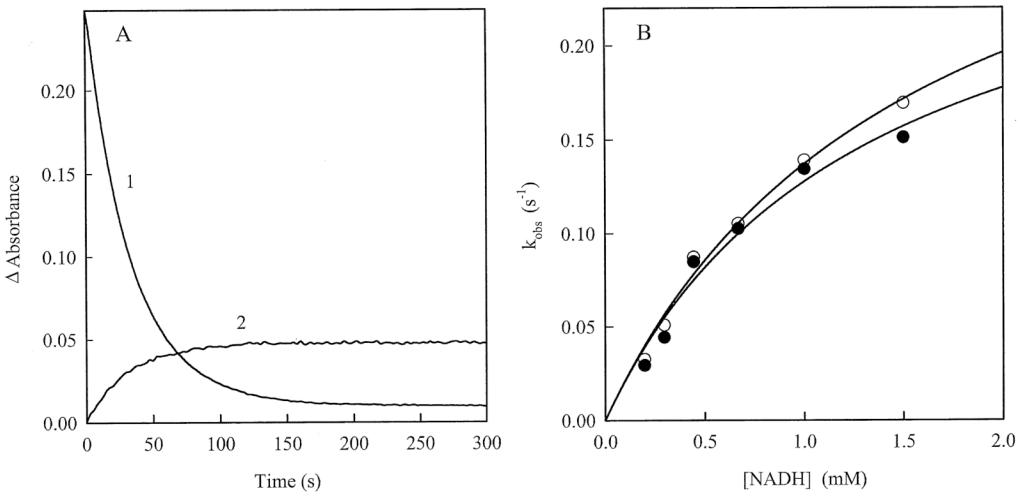

Fig. 5.

Pre-steady-state kinetics of AIF reduction by NADH. A) Kinetic traces of the absorbance change at 452 (1) and 700 nm (2) observed during reduction of 22 μM AIF by 200 μM NADH. The obtained first-order reduction rate constants were 0.034±0.002 s^{-1} (1) and 0.0372±0.027 s^{-1} (2). B) Dependence of the first-order rate constants for AIF reduction on the concentration of NADH in the absence (open circles) and presence of 5.0 mM NAD^+ (filled circles).

NIH-PA Author Manuscript

NIH-PA Author Manuscript

NIH-PA Author Manuscript

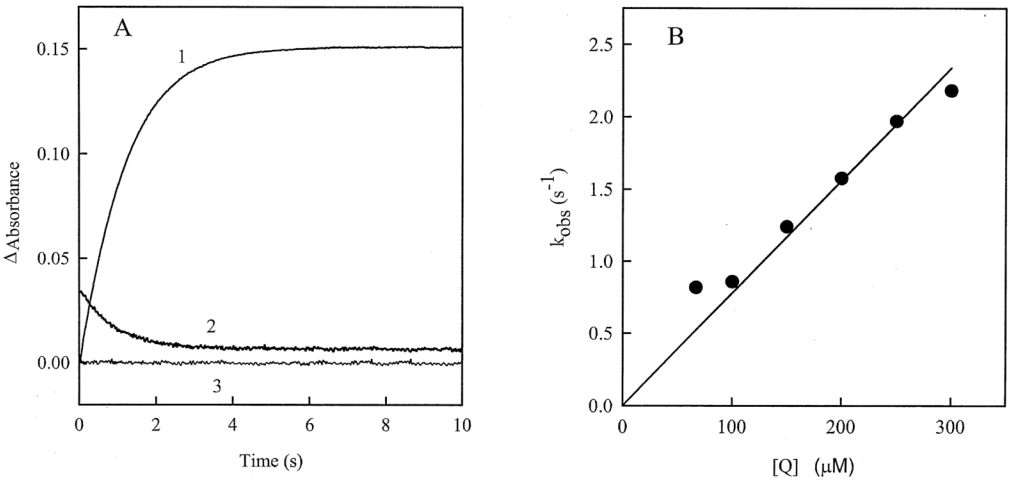

Fig. 6.

Pre-steady-state kinetics of AIF oxidation by 2,6-dimethyl-1,4-bezoquinone. A) Kinetic traces of the absorbance change at 452 (1,3) and 700 nm (2) during oxidation of 14 μM AIF by 100 μM 2,6-dimethyl-1,4-benzoquinone (1,2), or after mixing of reduced AIF with a pure buffer solution (3). The obtained first-order oxidation rate constants were 0.890±0.002 s^{-1} (1) and 1.013±0.012 s^{-1} (2). B) Dependence of the observed rate constant for AIF oxidation on the concentration of 2,6-dimethyl-1,4-benzoquinone.

NIH-PA Author Manuscript

NIH-PA Author Manuscript

NIH-PA Author Manuscript

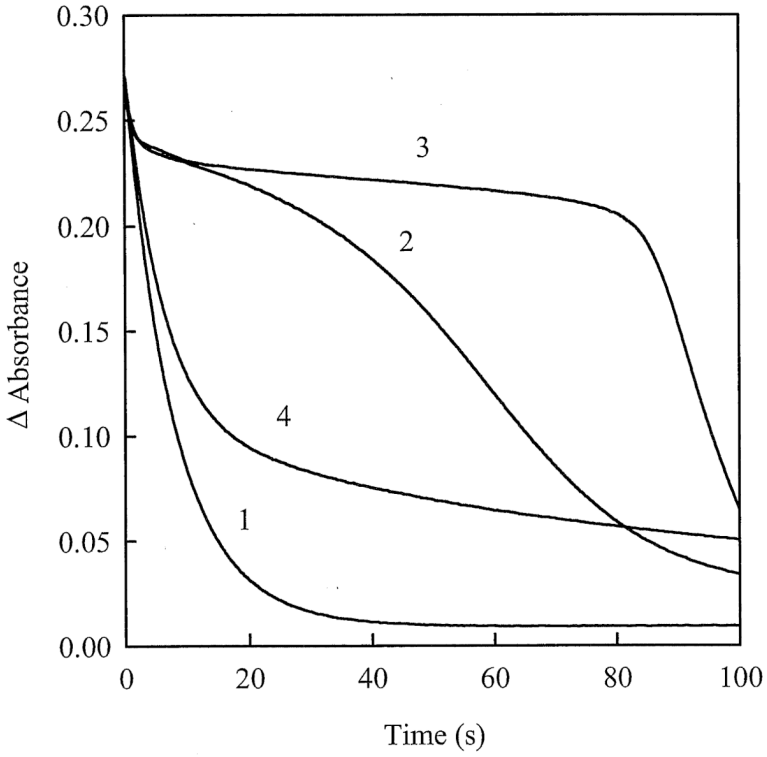

Fig. 7.

Reduction of 20 μM AIF with 1.0 mM NADH in the absence (1) and presence of 20 μM 2,6-dimethyl-1,4-benzoquinone (2), 5,8-dihydroxy-1,4-naphthoquinone (3), and RH1 (4). Kinetics of FAD reduction was monitored in 100 mM K-phosphate, pH 7.0, 1 mM EDTA at 452 nm and 25°C.

NIH-PA Author Manuscript

NIH-PA Author Manuscript

NIH-PA Author Manuscript

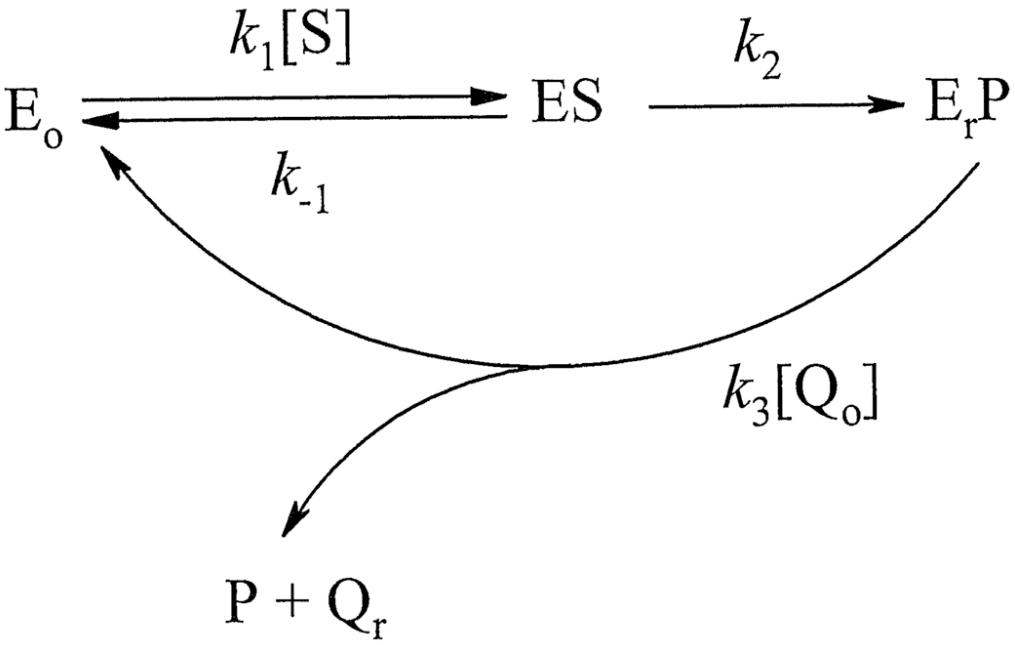

Scheme 1.

NIH-PA Author Manuscript NIH-PA Author Manuscript NIH-PA Author Manuscript

Arch Biochem Biophys. Author manuscript; available in PMC 2012 August 15.

Table 1

Molecular and redox properties of the quinoidal compounds

One-electron reduction potentials (E^1_7) and Van der Waals volumes (VdWvol) of the investigated quinones were determined previously [16-19]. The catalytic (k_{cat}) and second order (k_{cat}/K_m) rate constants for the AIF-catalyzed quinone reduction reactions were measured in the presence of 200 μM NADH as described in Materials and Methods.

No.	Compound	k_{cat}/K_m (M^{-1} s^{-1})	k_{cat} (s^{-1})	E^1_7 (V)	VdWvol (Å^3)
1.	1,4-Benzoquinone	$(7.6 \pm 0.8) \times 10^3$	0.030 ± 0.005	0.09	124
2.	2-Methyl-1,4-benzoquinone	$(7.3 \pm 0.7) \times 10^3$	0.041 ± 0.003	0.01	143
3.	2-*t*-Butyl-1,4-benzoquinone	$(1.3 \pm 0.1) \times 10^4$	0.040 ± 0.004	0.01	194
4.	2,5-Dimethyl-1,4-benzoquinone	$(2.9 \pm 0.4) \times 10^3$	0.030 ± 0.003	-0.07	161
5.	2,3-Dimethyl-1,4-benzoquinone	$(1.0 \pm 0.1) \times 10^4$	0.042 ± 0.002	-0.07	161
6.	2,6-Dimethyl-1,4-benzoquinone	$(1.2 \pm 0.2) \times 10^4$	0.044 ± 0.001	-0.07	161
7.	2,5-Bis(carboethoxyamino)- 3,6-diaziridinyl-1,4-benzoquinone (AZQ)	$(1.7 \pm 0.2) \times 10^3$	n.d.	-0.07	361
8.	2,5-Di-*t*-butyl-1,4-benzoquinone	$(1.2 \pm 0.1) \times 10^3$	0.025 ± 0.003	-0.08	264
9.	2,6-Di-*t*-butyl-1,4-benzoquinone	$(9.2 \pm 1.0) \times 10^2$	0.050 ± 0.004	-0.08	264
10.	5-Hydroxy-1,4-naphthoquinone	$(2.0 \pm 0.4) \times 10^3$	0.047 ± 0.003	-0.09	180
11.	5,8-Dihydroxy-1,4-naphthoquinone	$(3.9 \pm 0.3) \times 10^3$	0.044 ± 0.001	-0.11	192
12.	1,4-Naphthoquinone	$(1.5 \pm 0.2) \times 10^3$	0.037 ± 0.002	-0.15	168
13.	2-Methyl-5-hydroxy-1,4-naphthoquinone	$(1.1 \pm 0.1) \times 10^3$	0.041 ± 0.004	-0.16	200
14.	Trimethyl-1,4-benzoquinone	$(1.7 \pm 0.1) \times 10^3$	0.054 ± 0.003	-0.17	178
15.	2-Methyl-1,4-naphthoquinone	$(4.7 \pm 0.3) \times 10^2$	n.d.	-0.20	187
16.	2,5-Diaziridinyl -3-hydroxymethyl-6-methyl-1,4-benzoquinone (RH1)	$(4.3 \pm 0.1) \times 10^2$	n.d.	-0.23	247
17.	2,5-Dimethyl-3,6-diaziridinyl-1,4-benzoquinone (MeDZQ)	$(2.3 \pm 0.3) \times 10^3$	n.d.	-0.23	238
18.	1,4-Dihydroxy-9,10-anthraquinone	< 10	n.d.	-0.25	245
19.	Tetramethyl-1,4-benzoquinone	$(1.5 \pm 0.1) \times 10^2$	n.d.	-0.26	198
20.	1,8-Dihydroxy-9,10-anthraquinone	< 10	n.d.	-0.33	245
22.	Daunorubicin	< 10	n.d.	-0.34	600
23.	2,5-Bis(2-hydroxyethylamino)-3,6-diaziridinyl-1,4-benzoquinone (BZQ)	$(3.9 \pm 0.4) \times 10^1$	n.d.	-0.38	327
24.	2-Hydroxy-1,4-naphthoquinone	$(6.2 \pm 0.1) \times 10^1$	n.d.	-	

n.d. - not determined.